

**Manuscript version: Author's Accepted Manuscript**

The version presented in WRAP is the author's accepted manuscript and may differ from the published version or Version of Record.

**Persistent WRAP URL:**

<http://wrap.warwick.ac.uk/171847>

**How to cite:**

Please refer to published version for the most recent bibliographic citation information. If a published version is known of, the repository item page linked to above, will contain details on accessing it.

**Copyright and reuse:**

The Warwick Research Archive Portal (WRAP) makes this work by researchers of the University of Warwick available open access under the following conditions.

Copyright © and all moral rights to the version of the paper presented here belong to the individual author(s) and/or other copyright owners. To the extent reasonable and practicable the material made available in WRAP has been checked for eligibility before being made available.

Copies of full items can be used for personal research or study, educational, or not-for-profit purposes without prior permission or charge. Provided that the authors, title and full bibliographic details are credited, a hyperlink and/or URL is given for the original metadata page and the content is not changed in any way.

**Publisher's statement:**

Please refer to the repository item page, publisher's statement section, for further information.

For more information, please contact the WRAP Team at: [wrap@warwick.ac.uk](mailto:wrap@warwick.ac.uk).

# Numerical investigation of application of unidirectional generation to improve signal interpretation of circumferential guided waves in pipes for defect detection

Alan C. Kubrusly<sup>1</sup> [0000-0002-8633-4903], Lei Kang<sup>2</sup>, Jean Pierre von der Weid<sup>1</sup> and Steve Dixon<sup>3</sup>

<sup>1</sup> Centre for Telecommunication Studies, Pontifical Catholic University of Rio de Janeiro, 22451-900, Brazil (e-mail: alan@cpti.cetuc.puc-rio.br),

<sup>2</sup> School of Energy and Electronic Engineering, University of Portsmouth, PO1 3DJ, U.K.

<sup>3</sup> Department of Physics, University of Warwick, CV4 7AL, U.K

**Abstract.** Monitoring and inspection of pipes are paramount in several industry sectors. A convenient approach employs shear horizontal ultrasonic guided waves that propagate circumferentially around the pipe, known as CSH waves. Typically, a pair of transducers, a transmitter and a receiver, can be used to interrogate the whole circumference. Conventional shear horizontal transducers generate waves that propagate in both directions, namely, clockwise and counterclockwise. Bidirectional generation complicates the interpretation of the received signal since the scattered waves from a potential defect can mix themselves or with one of the two direct waves generated by the transmitter. In this paper, we address how unidirectional generation can ease the signal interpretation task for circumferential guided wave testing utilizing finite element simulations. Unidirectional generation is based on dual periodic elements transducer driven by phased pulses, following a design previously presented. Generation and reception were performed with separate transducers on the outer surface of a 324 mm outer diameter, 6.25 mm wall thickness steel pipe. Corrosion-like defects were modelled on the inner surface. We show that, when the angular position of the defect approaches 180° from the transmitter, the defect echo can be almost completely masked by the wave generated in the opposite direction. Unidirectional generation of CSH waves proves itself to be an important feature in pipeline integrity monitoring, providing more reliable signal interpretation.

**Keywords:** Circumferential guided waves, shear horizontal waves, unidirectional generation.

## 1 Introduction

Pipeline monitoring is paramount to detecting damages, such as corrosion and cracks [1-2]. Ultrasonic-based methods are widely used for material inspection and monitoring [3]. Plate-like and pipe-like structures support the propagation of ultrasonic guid-

ed waves (UGWs) [4]. UGWs propagate along the longitudinal coordinate being guided by the thickness of the sample. In pipes, one usually considers UGW that propagates either along the pipe's axis [5] or in the circumferential direction [6]. UGW is especially attractive for structural health monitoring (SHM) since a large area can be interrogated with a few transducers. For instance, longitudinal guided waves in pipes can propagate long distances, being able to carry information of the location of flaws in the axial direction, but with circumferential location being usually more complicated [7, 8]. On the other hand, circumferential guided waves can indicate the circumferential flaw location through the time-of-flight analysis [9, 10].

In flat plates, there are two well-defined families of guided waves in isotropic materials, namely, Lamb and shear horizontal (SH) waves. The latter has just one non-null displacement component, perpendicular to the cross-section and to the wave propagation direction and present advantages such as no energy leakage to non-viscous fluid loading, and allow one to operate at a single-mode regime when the frequency is relatively low [4]. SH guided waves are widely used to detect defects in plates and pipes [9-14]. Circumferential guided waves (CGW) can also be divided into circumferential SH (CSH) [15] or circumferential Lamb-type waves [4], which present similar propagation characteristics to their flat-plate counterparts.

In order to generate SH or CSH waves, one has to impose shear stress at the specimen surface, orthogonally to the generation direction. This can be performed with shear-polarized piezoelectric strips [16], magnetostrictive patch transducers [17] or periodic permanent magnet (PPM) electromagnetic acoustic transducers (EMAT) [18]. Those transducers, however, generate waves that propagate in both forward and backward travelling directions. In plates, this can be inconvenient, since the wave that propagates backwards can be eventually reflected and interfere with a signal of interest, from the wave that originally propagated in the forward direction. When propagating circumferentially around the closed propagation path of the pipe, the wave that is generated travelling in the unwanted direction, inexorably arrives at the receiver, either as a direct or scattered wave. Therefore, careful signal interpretation should be carried out, considering this inherent propagation complexity. An adopted strategy consists of using separated transmitter and receiver transducers, positioned and such a way to define short and long propagation paths, due to the simultaneous generation in both clockwise and counterclockwise directions, and establishing expected baseline signal for a defect-free pipe [11, 12].

Unidirectional generation of UGW can be achieved with two sets of sources separated in the longitudinal direction and driven by phase delayed pulses [19-21]. Chen et al. [19] used shear-polarized piezoelectric strips to generate SH waves in a single direction, and we presented two concepts of dual PPM-like EMATs that generate SH waves unidirectionally [20-21]. In this paper, we exploit the benefits of unidirectional generation of CSH waves for detecting defects in pipes through finite element simulations.

## 2 Circumferential SH waves and unidirectional generation

### 2.1 Circumferential SH waves

Shear horizontal guided waves present only one non-null displacement component, perpendicular to the propagation direction and to the plate or pipe surface. When guided circumferentially around a pipe, its wavefield is given by [4]:

$$u_z = A(r)e^{j(\omega t - p\theta)}, \quad (1)$$

where  $\omega$  is the angular frequency,  $p$  is the wavenumber in the angular direction,  $\theta$ , and  $A(r)$  is the mode's profile that depends on the radial coordinate  $r$ . The displacement wavefield is composed of a single component,  $u_z$ , which is polarized in the  $z$ -direction. There are potentially infinite CSH wave modes, which are given by the solution of its characteristic equation [15]. If the inner-to-outer-radius-ratio approaches unity, the exact pipe solution approaches the plate solution [15]. Here, we investigate a 324 mm outer diameter, 6.25 mm wall thickness mild steel pipe, in which the inner to outer radius ratio is 0.96, and thus the plate solution is a good approximation. In this case, the fundamental CSH0 mode is almost non-dispersive, and hence this mode is used hereinafter.

### 2.2 Unidirectional generation of SH waves

Either conventional PPM EMATs [18] or shear-polarized piezoelectric strips [16] generate SH waves that propagate in two opposite directions, namely, forward and backward, or clockwise and counterclockwise. **Fig. 1(a)** and **(b)** schematically shows the force pattern that can be imposed with the aforementioned transducers on the surface of a plate or pipe, respectively. The forces are polarized in the  $z$ -direction, and the propagation occurs in both positive and negative directions of the  $x$  or  $\theta$  axes, for plates or pipes, respectively. The separation between consecutive forces of alternate polarity defines half the nominal wavelength of the generated waves.

In order to generate SH waves in a single direction, one can use two sets of sources separated by a quarter wavelength, as shown in **Fig. 2(c)** and **(d)**, excited by pulses with a  $90^\circ$  phase difference between them on each transducer [19-21]. The spatial separation and phase shifts ensure that the waves generated by the two sets of sources constructively interfere in one direction, and destructively interfere in the opposite one, providing unidirectional generation [21]. This mechanism was used previously to unidirectionally generate SH waves in a single direction with a dual-PPM EMAT [20-21] or a dual array of shear-polarized piezoelectric strips [19].

It is worth noticing that by simply changing the phase shift between pulses from  $90^\circ$  to  $-90^\circ$ , one commutes the direction in which the waves propagate. For circumferential propagation, this is highly relevant since one can switch between clockwise and counterclockwise propagation in a convenient and simple way.

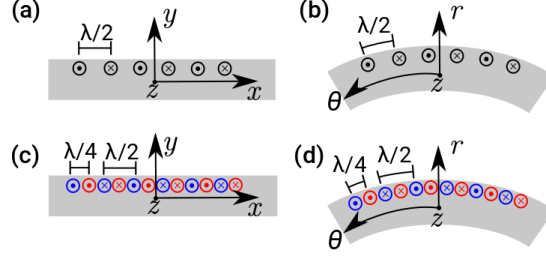


**Fig. 1.** Schematic representation of force pattern, in the  $z$ -direction, to generate SH waves in plates (a) and (c) and pipes (b) and (d). The symbol  $\odot$  means the force is pointing out of the page, and the symbol  $\otimes$  means the force is pointing inwards the page. The separation between consecutive forces of alternate polarity defines half the nominal wavelength of the generated waves. Single source (a) and (b), that generate SH waves in both directions of the  $x$  or  $\theta$  axes, and dual sources, red and blue symbols, (c) and (d), separated by a quarter wavelength that generated SH in a single direction or the  $x$  or  $\theta$  axes, when triggered by  $90^\circ$  phased pulses.

### 2.3 Reflection from a defect

The presence of a defect changes the received signal when compared to a non-defective pipe, due to wave scattering [13, 14]. The incident wave undergoes partial reflection, creating a new wavefront that propagates backwards, and partial transmission throughout the defect in the forward direction, which usually presents lower amplitude and altered waveform, when compared to the direct wave under the absence of a defect [13]. Due to the closed-loop propagation path of circumferential guided waves in pipes, bidirectional generation can considerably complicate signal interpretation, depending on the defect position. The received signal corresponding to the wave reflected from a defect can mix with the signal corresponding to the direct wave that propagates in the opposite direction.

This is schematically illustrated in **Fig. 2**, where orange and blue arrows represent the generated waves in the clockwise and counterclockwise directions, respectively, and red and magenta arrows represent the reflected wave from the defect due to clockwise and counterclockwise generation, respectively.  $Tx$  and  $Rx$  mean the transmitter and receiver, respectively. For the sake of simplicity, in **Fig. 2(a)** only the reflection from the clockwise travelling wave is shown, whereas in **Fig. 2(b)**, the reflection from the counterclockwise travelling wave is shown. The distance between transmitter and receiver is  $r$ , the distance from  $Tx$  to the defect in the clockwise and counterclockwise directions are  $s_{ckw}$  and  $s_{cckw}$ , respectively, and the pipe circumference is  $P$ .

Observing **Fig. 2(a)**, the reflection from the defect for the clockwise generated wave, orange-red arrow path, and the direct wave passing through the defect, which is generated in the opposite direction, blue arrow path, present, respectively, the following time-of-arrivals:

$$t_{ckw}^r = (2s_{ckw} - r)/c, \quad (2a)$$

$$t_{cckw}^t = (P - r)/c, \quad (2b)$$

where  $c$  is the wave mode propagating speed. As the angular position of the defect approaches  $180^\circ$  from the transmitter, both of the aforementioned time-of-arrivals approach each other. Indeed, if  $s_{ckw} = s_{cckw} = P/2$ , then  $t_{ckw}^r = t_{cckw}^r$ . This means that the echo from the defect can be masked by the wave that is generated and travels in the opposite direction, hindering signal interpretation. Note that this occurs independently of the position of the receiver.

The same holds for the echo from the defect originated from the longer path, due to counterclockwise generation. In **Fig. 2(b)**, it is represented the reflection from the defect for the counterclockwise generated wave, by the blue-magenta arrow path, and the second direct wave, which arrives after a complete wrap around trip and passing through the defect, that is generated in the opposite direction, by the orange arrow. Their theoretical time of arrivals are, respectively, given by

$$t_{cckw}^r = (2s_{cckw} + r)/c, \quad (3a)$$

$$t_{ckw}^t = (P + r)/c. \quad (3b)$$

Again, if  $s_{ckw} = s_{cckw} = P/2$ , then  $t_{cckw}^r = t_{ckw}^t$ .

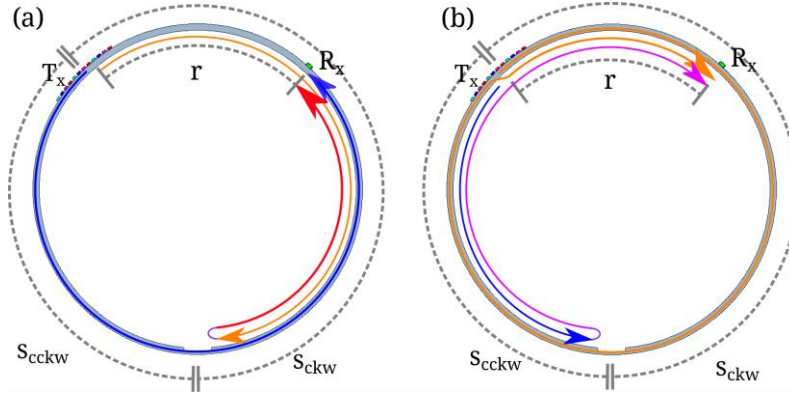


**Fig. 2.** Schematic representation of direct propagation through the defect in one direction and reflection from the defect in the opposite direction. In (a) only the reflection from the wave that initially travels in the clockwise generation is shown, and in (b) only the reflection from the wave that initially travels in the counterclockwise generation is shown.

### 3 Finite element model

In order to investigate the propagating characteristics of CSH in pipes under bidirectional and unidirectional generation, a commercial Finite Element solver was used. A 324 mm outer diameter, 6.25 mm wall thickness steel pipe was modelled, as shown in **Fig. 3(b)**. The transverse material wave speed was set to  $c_T = 3200\text{m/s}$ .

In order to generate the CSH waves, a set of sources that impose constant force densities were applied along the  $z$ -direction, following the pattern shown in **Fig. 1**, at

predefined regions on the surface of the model. Those can correspond to the generated forces of a PPM-like EMAT or shear-polarized piezoelectric strips. In order to form a dual-array, capable of generating a wave in a single direction, two independent arrays of sources were modelled in the outer surface of the pipe, and centred at the angular position of  $\theta=135^\circ$ , as shown in the detailed view of **Fig. 3(a)**. The coloured rectangles are shear sources, polarized in the  $z$ -direction. The red and blue rectangles correspond, respectively, to positive and negative forces of the first array; whereas magenta and cyan rectangles are the positive and negative forces, respectively, for the second array. Each array has three spatial cycles, the length of each element is 4 mm and the gap between elements is 2.2 mm thus providing a nominal wavelength of approximately  $\lambda=25$  mm.

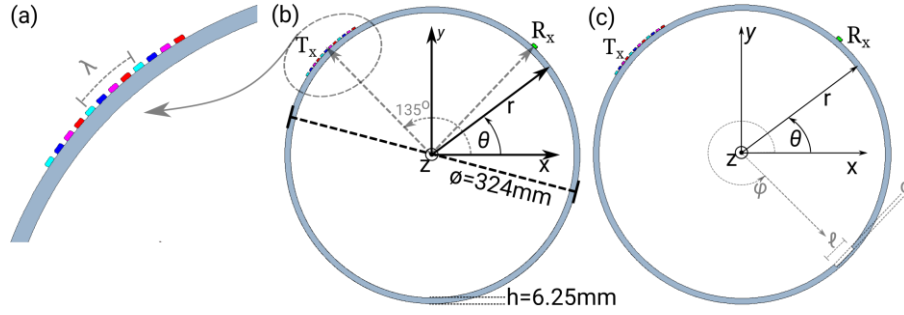


**Fig. 3.** Geometry of the modelled pipe. (a) Detail of SH wave generation area, centred at  $\theta=135^\circ$ . It consists of a dual-array with three spatial periods. (b) Non-defective 324 mm outer diameter, 6.25 mm wall thickness steel pipe with coordinate axes. (c) Pipe with an inner wall thinning defect centred at the angular coordinate  $\phi$ , with length  $\ell$  and depth  $d$ .

To generate the CSH0 wave, the excitation signal is set as a 3-cycle tone-burst, centred at 130 kHz. Following section 2.2, unidirectional generation in the clockwise direction is obtained when the pulse applied to the first array is delayed by  $90^\circ$  with respect to the second array, whilst if the pulse applied to the second array is delayed by  $90^\circ$  with respect to the first array, counterclockwise propagation occurs. If no delay is used, and thus the applied signals at both arrays are the same, bidirectional generation takes place. The green rectangle in **Fig. 3(b)** represents a single-element receiver, positioned at  $\theta=45^\circ$ , thus  $90^\circ$  to the clockwise direction from the transmitter.

In addition to a defect-free pipe, models with wall thinning, which crudely mimics an inner corrosion defect, were also simulated, as shown in **Fig. 3(c)**. The defect depth was set to half thickness,  $d=h/2$ , its length was set to  $\ell=27$ mm, corresponding to  $10^\circ$  extension, and the angular position of its centre, defined as angle  $\phi$ , was varied.

## 4 Results and discussion

**Fig. 4** illustrates the interaction with a defect, positioned at the angular position of  $\phi=270^\circ$ , by means of snapshots of the wavefield. In **Fig. 4(a)-(c)** the time instant is  $t=44$   $\mu$ s, just after being generated and prior to any interaction. In **Fig. 4(d)-(e)** time

instant is  $t = 229 \mu\text{s}$ , after interaction with the defect. In **Fig. 4(a)** and (d), no delay is applied to both arrays, whereas **Fig. 4 (b)** and (e) show generation when a delay of  $90^\circ$  is applied to the first array and **Fig. 4 (c)** and (f) with a  $-90^\circ$  delay. In **Fig. 4(a)** two wavefronts are generated and propagate in both directions, whilst with the adequate time-delay, **Fig. 4 (b)** and (c), effectively unidirectional generation in the direction of interest is achieved. As can be seen in **Fig. 4(d)**, bidirectional generation creates four wavefronts after the first interaction with the defect, being two reflected and two transmitted ones. On the other hand, with unidirectional generation as shown in **Fig. 4(e)** and (f), there is only one reflected and one transmitted wave for a single propagation loop, therefore simplifying the received signal.

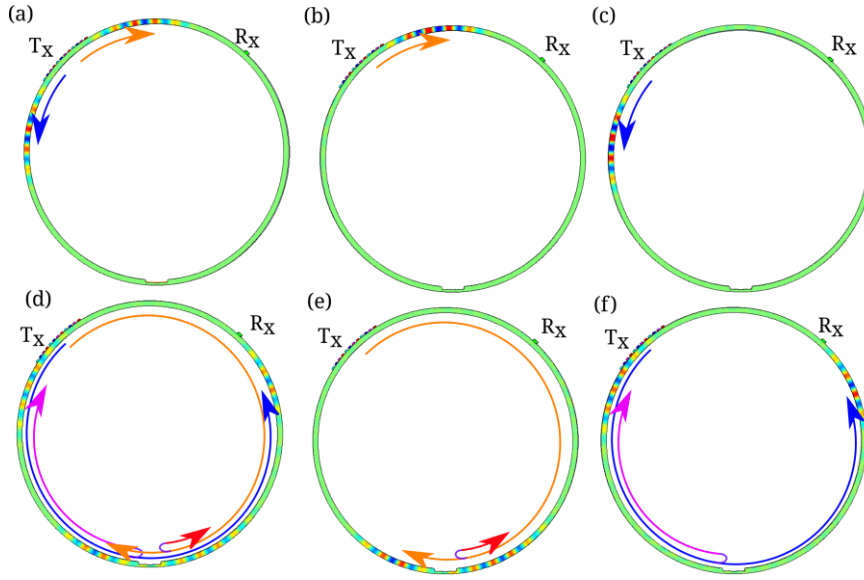


**Fig. 4.** Snapshots of the SH wavefield in a pipe with half-thickness deep wall-thinning defect positioned at the angular position of  $270^\circ$  for time  $t = 44 \mu\text{s}$  (a)-(c), and  $t = 229 \mu\text{s}$  (d)-(f) for bidirectional generation (a) and (d), unidirectional generation in the clockwise direction (b) and (e) and in the counterclockwise direction, (c) and (f). Tx and Rx mean the transmitter and receiver, respectively. The orange and blue arrows represent the clockwise and counterclockwise propagation directions.

The dependence of the defect position in the signal received at Rx,  $u$ , is shown **Fig. 5**, when the defect is positioned in three distinct angular positions. These positions are  $270^\circ$  (as illustrated in **Fig. 4**) and shown here in Fig. 5(a)-(c),  $292.5^\circ$  as shown in Fig. 5(d)-(f), and at  $315^\circ$  ( $180^\circ$  from the transmitter, thus imposing  $s_{ckw} = s_{cckw} = P/2$ ) as shown in Fig. 5 (g)-(i). In all the plots of Fig. 5, the received signal under the absence of a defect is shown by the black line, for the sake of comparison.



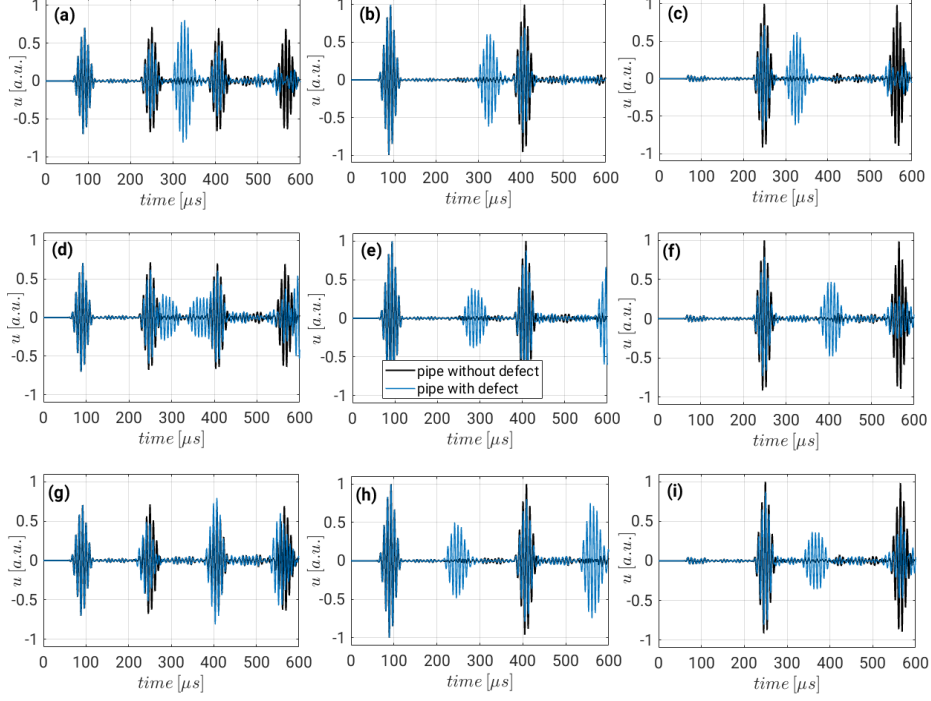


**Fig. 5.** Numerically simulated received signals,  $u$ , of circumferential shear horizontal waves in a 324 mm outer diameter, 6.25 mm thick steel pipe without any defect (black line) and with a 27 mm long, half-thickness deep wall-thinning defect (blue line) positioned at the angular position of  $270^\circ$  (a)-(c),  $292.5^\circ$  (d)-(f), and  $315^\circ$  (which means  $180^\circ$  from the transmitter) (g)-(i). The receiver is positioned  $90^\circ$  in the clockwise direction from the transmitter. Conventional bidirectional generation (a), (d), (g), unidirectional generation to the clockwise direction (b), (e), (h) and counterclockwise direction (c), (f), (i).

In **Fig. 5(a)-(c)**, one can see that the echo from the defect arrives at about  $300 \mu\text{s}$  and is identifiable even under bidirectional generation, despite being amongst several pulses. Therefore, a baseline comparison with the non-defective case is still feasible and straightforward even under bidirectional generation.

In **Fig. 5(d)-(f)**, the defect approaches the angular position, in which it is at  $180^\circ$  from the transmitter. The time of arrival of the echoes from the defect approaches the time of arrival of the directed wave generated in the opposite direction, as can be seen in **Fig. 5(d)**. With unidirectional generation, **Fig. 5(e)-(f)**, a clearer echo identification is possible.

In **Fig. 5(g)-(i)** the defect is exactly at  $180^\circ$  from the transmitter. Note that the echo from the defect arrives at  $250 \mu\text{s}$ , when the wave is generated in the clockwise direction and at  $400 \mu\text{s}$  when it is generated in the counterclockwise direction. As theoretically predicted in Section 2.3, those are exactly the same time at which the direct wave that propagates in the opposite direction arrives, after passing through the de-

fect. Hence, with bidirectional generation, the defect echoes are completely masked by direct waves, as can be verified in **Fig. 5(g)**, and are quite similar to a baseline defect-free case. On the other hand, the defect echoes can be clearly identifiable with unidirectional generation, **Fig. 5(h)-(i)**, making defect detection possible and straightforward.

## 5 Conclusion

SH guided wave propagating circumferentially around a pipe is useful to detect defects such as corrosion. The usual SH wave transduction mechanisms generate SH guided waves in two main directions. For circumferential guided waves, this means that twice as many wavefronts are potentially detectable due to the wrap-around propagation of the waves generated in both directions, and those can mix with a potential scattered wave of interest. Unidirectional generation of SH guided waves can be achieved with two sets of forces separated in the longitudinal direction and triggered with the adequate time delay, as used before with either PPM EMATs or shear-polarized piezoelectric strips. With the aid of finite element analysis, we have shown that unidirectional generation can significantly simplify signal analysis, by effectively suppressing the wave generated to the unwanted direction. In particular, we proved that when the angular position of the defect approaches  $180^\circ$  from the transmitter, the defect echo is almost completely masked by the wave generated in the opposite direction, which is suppressed with unidirectional generation, and thus clearly reveals a defect echo. Additionally, switching between clockwise and counterclockwise travelling wave generation, which can be simply performed by changing the time-delay excitation, allows one to obtain clearer information on a potential reflector. Unidirectional generation of CSH waves is an important feature in pipeline monitoring, providing more reliable signal interpretation.

## Acknowledgments

This study was financed in part by the Coordenação de Aperfeiçoamento de Pessoal de Nível Superior - Brasil (CAPES) - Finance Code 001, by the Carlos Chagas Filho Foundation for Research Support of Rio de Janeiro State (FAPERJ) and by the Brazilian National Council for Scientific and Technological Development (CNPq).

## References

1. R. F. Wright, P. Lu, J. Devkota, F. Lu, M. Ziomek-Moroz and P. R. Ohodnicki Jr., "Corrosion Sensors for Structural Health Monitoring of Oil and Natural Gas Infrastructure: A Review," *Sensors*, vol. 19, no. 18, 2019.
2. M. Ho, S. El-Borgi, D. Patil and G. Song, "Inspection and monitoring systems subsea pipelines: A review paper," *Structural Health Monitoring*, vol. 19, no. 2, pp. 606-645, 2020.

3. M. Mitra and S. Golpalakrishnan, "Guided wave based structural health monitoring: A review," *Smart Materials and Structures*, vol. 25, no. 5, p. 053001, 2016.
4. J. L. Rose, *Ultrasonic Guided waves in solid media*, Cambridge University Press, 2014.
5. D. Gazis, "Three-Dimensional Investigation of the Propagation of Waves in Hollow Circular Cylinder. I. Analytical Foundation," *The Journal of the Acoustical Society of America*, vol. 31, no. 5, 1959.
6. G. Lui and J. Qu, "Guided circumferential waves in a circular annulus," *Journal of Applied Mechanics*, vol. 65, pp. 424-430, 1998.
7. M. J. S. Lowe, D. N. Alleyne and P. Cawley, "Defect detection in pipes using guided waves," *Ultrasonics*, vol. 36, no. 1-5, pp. 147-154, 1998.
8. A. Ghavamian, F. Mustapha, B. T. H. T. Baharudin and N. Yidris, "Detection, Localisation and Assessment of Defects in Pipes Using Guided Wave Techniques: A Review," *Sensors*, vol. 18, p. 4470, 2018.
9. H. Zhang, Y. Du, J. Tang, G. Kang and H. Miao, "Circumferential SH Wave Piezoelectric Transducer System for Monitoring Corrosion-Like Defect in Large-Diameter Pipes," *Sensors*, vol. 20, p. 460, 2020.
10. W. Shi, W. Chen, C. Lu and Y. Chen, "Interaction of circumferential SH<sub>0</sub> guided wave with circumferential cracks in pipelines," *Nondestructive Testing and Evaluation*, vol. 36, no. 5, pp. 571--596, 2021.
11. M. Clough, M. Fleming and S. Dixon, "Circumferential guided wave EMAT system for pipeline screening using shear horizontal ultrasound," *NDT & E International*, vol. 86, pp. 20-27, 2017.
12. B. Ren and J. Xin, "In-line inspection of unpiggable buried live gas pipes using circumferential EMAT guided waves," in *AIP Conference Proceedings* 1949, 020019, 2018.
13. A. C. Kubrusly, M. A. Freitas, J. P. von der Weid and S. Dixon, "Interaction of SH guided waves with wall thinning," *NDT & E International*, vol. 101, pp. 94-103, 2019.
14. A. C. Kubrusly and S. Dixon, "Application of the reciprocity principle to evaluation of mode-converted scattered shear horizontal (SH) wavefields in tapered thinning plates," *Ultrasonics*, vol. 117, p. 106544, 2021.
15. X. Zhao and J. L. Rose, "Guided circumferential shear horizontal waves in an isotropic hollow cylinder," *The Journal of the Acoustical Society of America*, vol. 115, no. 5, pp. 1912-1916, 2004.
16. H. Miao, Q. Huan, F. Li and G. Kang, "A variable-frequency bidirectional shear horizontal (SH) wave transducer based on dual face-shear (d24) piezoelectric wafers," *Ultrasonics*, vol. 89, pp. 13-21, 2018.
17. Y. Y. Kim and K. Y. E, "Review of magnetostrictive patch transducers and applications in ultrasonic nondestructive testing of waveguide," *Ultrasonics*, vol. 62, pp. 3-19, 2015.
18. P. A. Petcher, S. E. Burrows and S. Dixon, "Shear horizontal (SH) ultrasound wave propagation around smooth corners," *Ultrasonics*, vol. 54, no. 4, pp. 997-1004, 2014.
19. M. Chen, Q. Huan and F. Li, "A unidirectional SH wave transducer based on phase-controlled antiparallel thickness-shear (d15) piezoelectric strips," *Theor. Appl. Mech. Lett.*, vol. 10, no. 5, pp. 299-306, 2020.
20. A. C. Kubrusly, L. Kang and S. Dixon, "Unidirectional shear horizontal wave generation with side-shifted periodic permanent magnets electromagnetic acoustic transducer," *IEEE Trans. Ultrason., Ferroelectr., Freq.*, vol. 67, no. 12, pp. 2757-2760, 2020.
21. A. C. Kubrusly, L. Kang, I. S. Martins and S. Dixon, "Unidirectional Shear Horizontal Wave Generation by Periodic Permanent Magnets Electromagnetic Acoustic Transducer With Dual Linear-Coil Array," *IEEE Trans. Ultrason., Ferroelectr., Freq.*, vol. 68, no. 10, pp. 3135-3142, 2021.